Biointerface

Faculty of Medicine

The Fetuin Family

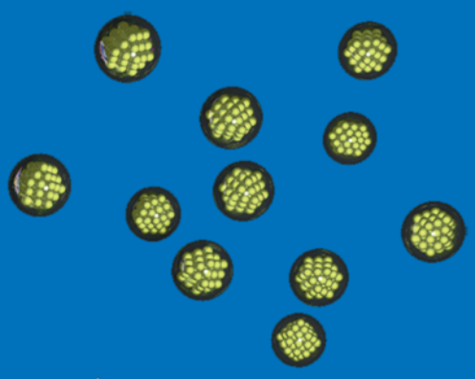

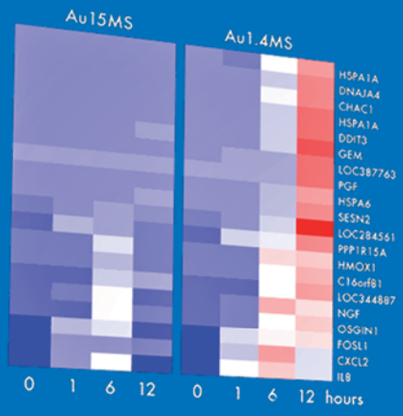

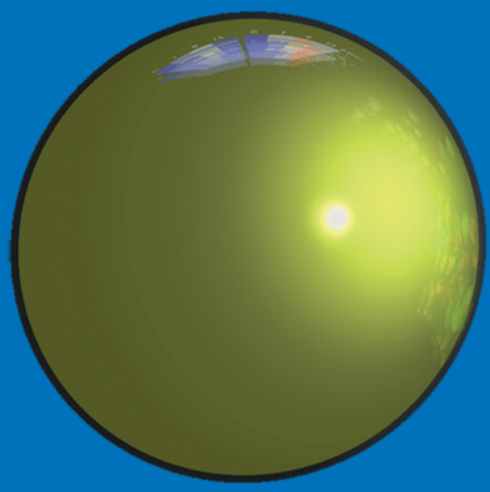

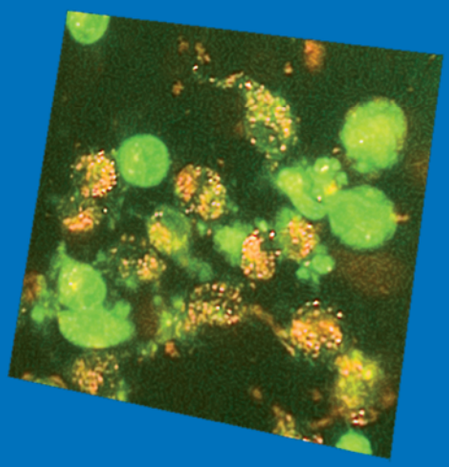

Director

Univ.-Prof. Dr. rer. nat.
Wilhelm Jahnen-Dechent

RWTH Aachen University Hospital
Pauwelsstrasse 30, D-52074 Aachen

Helmholtz-Institute for Biomedical Engineering
Pauwelsstrasse 20

Phone: +49 (0)241 80-80163 (Office)
+49 (0)241 80-80157 (Secretary)
Fax: +49 (0)241 80-82573
Email: rsous@ukaachen.de
Web: http://www.biointerface.rwth-aachen.de

Staff

Sous, Renate, Administrative Assistant

Dietzel, Eileen, B.Sc.
Dreymüller, Daniela, Dr. rer. nat.
Duarte-Campos, Daniela Filipa, M.Sc.
(Univ. Minho Portugal)
Farese, Stefan, Dr. med.
(University Berne, Switzerland)
Ferreira de Sousa, Rafael Simão, M.Sc.
(Univ. Minho Portugal)
Floehr, Julia, B.Sc.
Gräber, Steffen, CTA
Herrmann, Marietta, Dipl.-Biol.
Kinkeldey, Anne, Dipl. Biol.
Ludvigsen, Rebecca, B. Sc.
(Fulbright student)
Pan, Yu, M.Sc.
Schäfer, Cora, Dr. rer. nat.
Schepers, Jenny, B.Sc.

Cover: Gold nanoparticles (AuNPs) of 1.4-nm-diameter capped with triphenylphosphine monosulfonate (Au1.4MS) are much more cytotoxic than 15-nm nanoparticles (Au15MS). These toxic particles generate oxidative stress in cells, visible by leaky mitochondria (green monomeric JC-1 stain in the micrograph), and lead to necrosis. Furthermore, they up-regulate heat shock and stress-related genes, depicted by red bars in the heat-map representation of a gene chip analysis. AuNP illustration by Michael Noyong, Inorganic Chemistry, RWTH Aachen.

Introduction

The Biointerface Laboratory continues to work on the structure and function of secreted (type 3) cystatin protein family members, the fetuins (fetuin-A and fetuin-B) and histidine-rich glycoprotein (HRG) [1]. Cystatins (inhibitors of cysteine proteases) were identified in the 1960s. Since then, the cystatin family has been divided into type 1 (mainly intracellular proteins), type 2 (mainly extracellular proteins), and type 3 cystatins (plasma proteins). The cystatins inhibit cysteine peptidases of the papain family and play key roles in a wide array of physiological processes as well as in disease. The type 3 family members fetuin-A/alpha-2-Heremans Schmid (HS)-glycoprotein (AHSG), fetuin-B (FETUB), kininogen (KNG) and histidine-rich glycoprotein (HRG) are disulfide-bonded, multi-domain proteins with more than one cystatin-like domain; fetuin-A, fetuin-B and HRG each contain two tandem cystatin domains, whereas KNG contains three cystatin domains. Kininogen displays cystatin-activity whereas the other type 3 family members appear not to be functional cystatins. On the contrary, fetuin-A has been identified as a potential positive regulator of the cysteine protease m-calpain in wounded cells.

Alpha-2-HS-glycoprotein/fetuin-A	
1.	Approved name: Alpha-2HS-glycoprotein
	Also denoted fetuin-A
2.	Approved symbol: AHSG
3.	Accesion no: P02765
Fetuin-B	
1.	Approved name: fetuin-B
2.	Approved symbol: FETUB
3.	Accesion no: Q9UGM5
Kininogen	
1.	Approved name: kininogen
2.	Approved symbol: KNG
3.	Accesion no: P01042
Histidine-rich glycoprotein	
1.	Approved name: histidine-rich glycoprotein
2.	Approved symbol: HRG
3.	Accesion no: P04196

Table 1: Approved symbols for genes and proteins.

The type 3 members are glycoproteins secreted by the liver into the blood. Especially high concentrations occur during fetal life [2], hence the name fetuin, which was derived from the latin word fetus. Fetuin-A has its major role in regulation of mineralization [3, 4]. Fetuin-B has a similar tissue distribution as AHSG and the two proteins are co-regulated, possibly suggesting overlapping functions [5]. Both fetuin-A and fetuin-B have been implicated in the regulation of tumor growth. Kininogen is produced as several splice variants, high and low molecular weight KNG (HK and LK respectively), from which the hormone bradykinin is generated. Bradykinin is a potent inflammatory mediator that causes vasodilatation and enhanced capillary permeability. HRG is also important in regulation of clotting and fibrinolysis [6]. In addition to their function in regulation of coagulation, KNG and HRG serve as regulators of angiogenesis [7].

Chromosomal Localization and Gene Organization

The cystatin type 3 proteins are encoded by single-copy genes. The AHSG and FETUB genes are positioned immediately adjacent to the KNG and HRG genes on mouse chromosome 16 and human chromosome 3 (3q27) (Fig. 1).

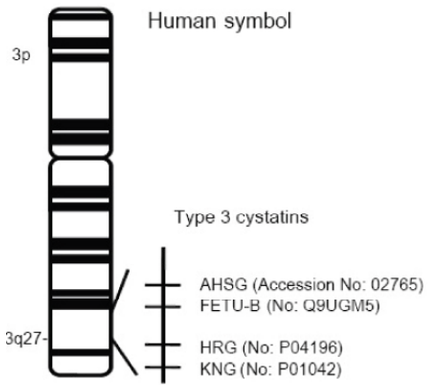

Fig. 1: Chromosomal organisation of cystatin type 3 proteins on human chromosome 3.

The human AHSG gene encompasses 7 exons spanning around 8.2 kb. Two common single nucleotide polymorphisms (SNPs) have been detected in the human; 6826C/T in exon 6 and 7495C/G in exon 7, which modulate circulating serum levels of AHSG.
The mouse FETUB gene consists of eight exons. The coding sequence starts in exon 2. Two alternative first exons encoding distinct 5'UTRs exist and have been denoted isoforms 1 and 3. Isoform 2 uses the same 5'UTR as isoform 1, but isoform 2 lacks exon 2 due to alternative splicing. These data have been derived from in silico cloning and await experimental confirmation. Thus, the physiological role of the putative splice variants is unclear.
The human HRG gene comprises 7 exons encompassing 12 kb. Notably, the largest exon VII encodes the entire C-terminal half of HRG. There are no HRG splice variants. Two different molecular weight forms, 75 and 77 kDa, of HRG in human blood samples have been described. The 77 kDa variant contains a serine residue at position 186, allowing attachment of an N-linked carbohydrate group. The 75 kDa form instead carries a proline at position 186. Three cases of congenital deficiency of HRG with familiar thrombophilia have been reported. All thrombophilic probands are women and their plasma HRG level is 20-50% of normal level. Two Japanese cases have been denoted Tokushima 1 and 2. The Tokushima 1 HRG variant contains a mutation resulting in exchange of Gly to Glu at position 85 in the first cystatin domain, which causes enhanced intracellular degradation of HRG. In the Tokushima 2 HRG, a mutation resulting in exchange of Cys to Arg at position 223 in the second cystatin domain has been identified.

Structure of Type 3 Cystatins

The type 3 cystatins are multi-domain proteins containing aminoterminal cystatin domains (Fig. 2). At this point, none of these proteins have been analyzed by X-ray crystallography, but computer modeling of the cystatin domains have been presented.

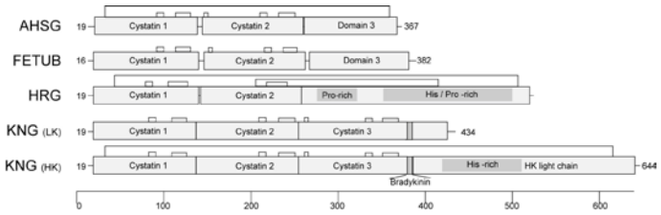

Fig. 2: Schematic structures of type 3 cystatins. Domain organization is shown with indications of disulfide bridges, cystatin domains, and the His/Gly and His/Pro domains in KNG and HRG, respectively.

Post-translational modifications are common in the type 3 cystatins. Fig. 3 illustrates post-translational modifications and binding motifs in AHSG, which is produced as a single chain precursor. The precursor is proteolytically processed to yield the mature circulating plasma form of AHSG comprising a heavy and a light chain. This first cleavage occurs by a secretory protein Golgi protease concomitantly with Ser/Thr phosphorylation and addition of N-linked carbohydrate groups. Proteolysis in septicemia can cleave another 40 amino acids from the C-terminus of the heavy chain, forming the so-called A-chain. The 40 amino acid residue C-terminal stretch has been termed "the connecting peptide" as it connects the combined A- and B-chains to the contiguous translated cDNA sequence.

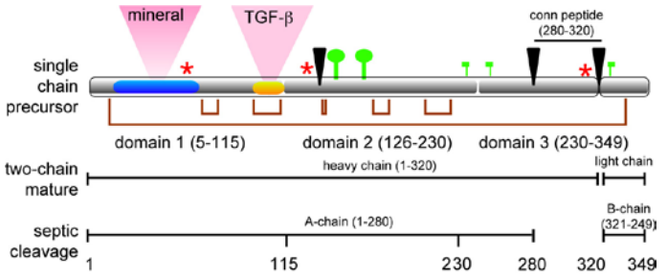

Fig. 3: Post-translational modification of AHSG, a prototypic type 3 cystatin family member. AHSG consists of three domains, D1-D3, of ~115 amino acids each. Disulfide bridges indicated in brown rectangles are characteristic of the tandemly arranged cystatin domains D1 and D2. One interdomain disulfide links domain D3 to domain D1. Proteolytic cleavage sites are indicated by black wedges, serine phosphorylation sites are marked as red asterisks, N-glycosylation sites as large green and O- glycosylation sites as small green beacons. The so-called connecting peptide of AHSG is indicated. Binding regions for apatite and TGF-ß like growth factors are shown as pink triangles. Please note that carbohydrate binding proteins and phosphoamino acid-specific ligands may also bind and influence AHSG activity and stability.

A substantial fraction of AHSG isolated from human plasma is serine phosphorylated; serine phosphorylation of AHSG has been implicated in its negative regulation of the insulin receptor tyrosine kinase but seems dispensable for the ability of AHSG to regulate mineralization. It is likely that these many post-translational modifications, which have been identified in human as well as bovine AHSG, may regulate activity, tissue targeting and plasma half-life.

Fetuin proteins occur in all vertebrates. Fig. 4 shows that Fetuins and HRG are predominantly made in the liver. Throughout fetal development of both zebrafish and mice the liver shows by far the strongest signal by *in situ* hybridization probing for fetuin homologues. Extrahepatic synthesis exist, but a conservative estimate suggests that more than 95% of the circulating levels of fetuin-A, fetuin-B and HRG are liver-derived.

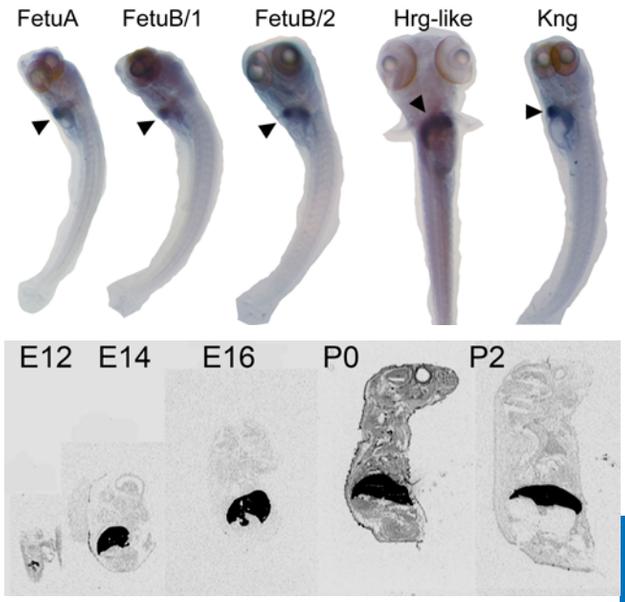

Fig. 4: Expression pattern of type 3 cystatins. Expression of type 3 cystatin family members in Danio rerio (zebrafish) at day 11 post fertilization (day 4 post-fertilization for HRG-like) (top) and (bottom) AHSG expression in the mouse, judged from in situ hybridization of developing (E, embryonic day) embryos as well as post partum (P) animals. Note the dominating expression of AHSG in the liver. The zebrafish genome harbours seven type 3 cystatin genes. The top shows in situ hybridizations with probes synthesized to correspond to nucleotide sequences homologous to the indicated gene names. The arrowheads indicate expression in the liver.

We study the biological function of fetuins and HRG by gene knockout in mice. We have generated gene knockouts for all three proteins and we maintain the genetically modified mice on various genetic backgrounds and in combination with related gene knockouts. Fetuin familiy proteins are prototypic carrier proteins with high surface activity. Their common core structure consisting of two cystatin-like protein domains each confers stability. Variations in the domain composition and in the three-dimensional structure confer specific biological activity mediated by molecular binding. Our latest work with knockout mice showed that the combination of gene knockouts can mimic complex diseases.

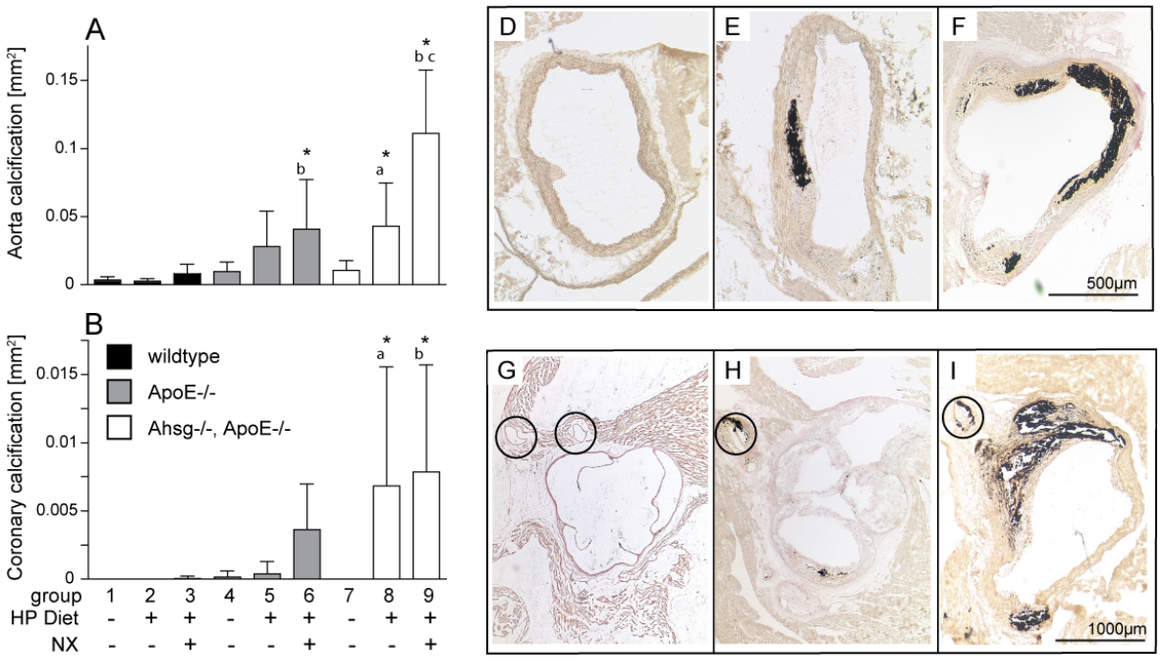

Fig. 5: (A) Vascular calcification histomorphometry of von Kossa–stained tissue sections of aorta calcification, (B) coronary artery calcification in the various treatment groups of wt (black), ApoE-/- (grey), and Ahsg-/-/ApoE-/- (white) mice. (D through I) Representative photomicrographs are depicted on the right for the treatment groups 3 (D and G), 6 (E and H), and 9 (F and I).

Fetuin-A protects against Atherosclerotic Calcification in a Model of Chronic Kidney Disease

Accelerated atherosclerosis in patients with chronic kidney disease is characterized by severe vascular calcification and the magnitude of calcification is associated with increased cardiovascular and all-cause mortality. Fetuin-A is an abundant liver-derived plasma protein and a particularly potent systemic inhibitor of soft tissue calcification [8]. Interestingly, and in contrast to humans, fetuin-A deficient mice spontaneously develop widespread soft tissue calcification, including significant myocardial calcification, but larger arteries are spared. This absence of vascular calcification compared to humans with calcification-associated diseases may result from the protection of an intact endothelium, which becomes severely compromised in the setting of atherosclerosis. To investigate this, we generated fetuin-A and apolipoprotein-E (ApoE) deficient mice and compared them with single ApoE deficient mice and wildtype mice. Three different treatment groups were investigated (1) standard diet, untreated, (2) high-phosphate diet to induce calcification stress and (3) unilateral nephrectomy (causing chronic kidney disease) plus high- phosphate diet. Fig. 5 summarizes the results of these experiments; fetuin-A deficiency did not affect the extent of aortic lipid deposition, neointima formation, and coronary sclerosis observed with ApoE deficiency, but the combination of fetuin-A deficiency, hyperphosphatemia, and CKD led to a 15-fold increase in vascular calcification in this model of atherosclerosis [3]. Thus a model of combined fetuin-A and ApoE deficiency shows a compound phenotype of increased atherogenesis and calcification.

Fetuin-A mediates the Binding and Uptake of Calciprotein Particles in Macrophages

Fetuin-A mediates the formation and stabilization of calciprotein particles (CPPs). Thus CPPs solubilize calcium and phosphate within the serum and consequently prevent ectopic mineralization. The clearing of CPPs from the blood flow has not been studied. CPPs have a size of about 200 nm [9], therefore they are most likely cleared by cells of the reticulo-endothelial system. We studied the uptake of fluorescence-labeled Fetuin-A and CPPs in different macrophage populations; bone marrow macrophages representing resident blood-borne macrophages and peritoneal macrophages as a model of inflammatory macrophages. We focused on a receptor-mediated uptake mechanism, which relies on binding at low temperature as illustrated (Fig. 6).

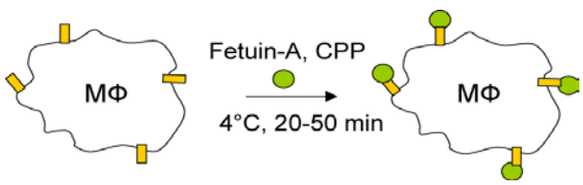

Fig. 6: Binding of fluorescence labeled Fetuin-A monomer or CPP lights up macrophages in flow cytometry

Incubation of the cells on ice prevents phagocytic activity and strictly measures binding of particles to the cell surface receptors. Cell-bound CPPs were quantified by flow cytometry as shown in Fig. 7. Intriguingly, fetuin-A containing CPPs bound to macrophages very avidly whereas

fetuin-A monomer did not. Thus CPP binding and uptake was mediated by a resident surface receptor present on both non-inflammatory bone marrow-derived macrophages and inflammatory peritoneal macrophages (Fig. 7C and D). Further characterization of this receptor is under way.

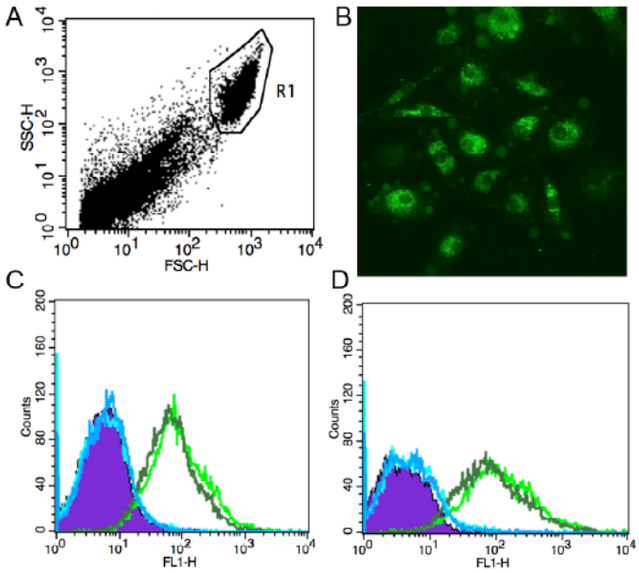

Fig. 7: Binding of CPPs shown by flow cytometry and fluorescence microscopy. A) Bone marrow macrophages were selected in area R1. B) Fluorescence picture of macrophages with ingested fluorescence-labeled CPPs. C) Cell associated fluorescence signal increases when bone marrow macrophages are incubated with CPPs (green curve), but not with Fetuin-A monomer (blue curve) in contrast to untreated cells (purple curve). D) as C) but with peritoneal macrophages.

In vivo Imaging of Calcification

Fluorescence Molecular Tomography (FMT) provides a non-invasive imaging method in mice and possibly in humans. In close cooperation with our colleagues from the Institute of Experimental Molecular Imaging, ExMi (head: Prof. Fabian Kiessling) we employed OsteoSense 680® to detect calcification in C57BL/6 Apolipoprotein E / Fetuin-A double deficient mice; these mice calcify in their aorta and also in their soft tissues. We employed the "3D mode" of the FMT scanner to detect enhanced fluorescence in the spine, in the kidneys, and the lung. Live animals can be imaged with mm resolution and centimeter penetration depth. Fig. 8 illustrates a typical 3D FMT scanning suggesting that active bone formation and calcification take place in the spine, the kidneys and the lung.

For higher resolution studies, we applied the so-called 2D scanning mode (reflectance image) to study calcification in explanted organs and tissues; the strongest fluorescence signals were detected in the kidneys and in the liver (Fig. 9). Judged against the size of the particular organ under study, we determined that the kidneys, followed by the liver and the lung, show the highest enrichment of OsteoSense 680® confirming that these organs are prone to calcification.

In conclusion, FMT is a valuable tool to study calcification *in vivo* and in real time; small animals like our knockout mice allow to further detail the calcification process by studying the contribution of individual gene products in a complex experimental setting mimicking human disease.

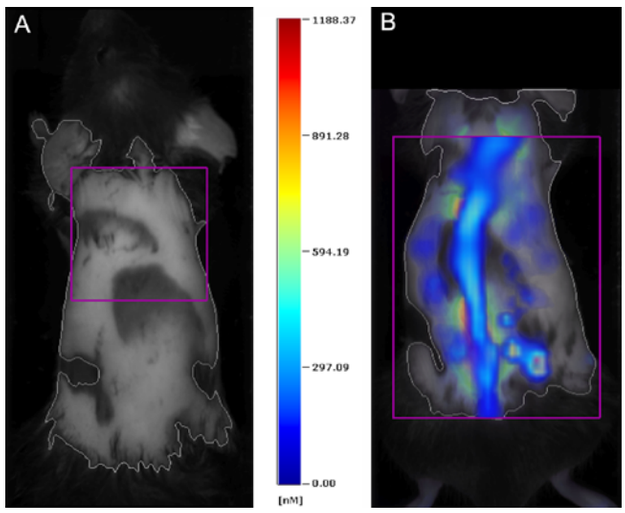

Fig. 8: In vivo FMT of an ApoE/FetA-/- mouse. A) shows a baseline measurement before injection of OsteoSense 680®. No fluorescence signal was detected. B) FMT analysis of the same animal 24 h after injection of OsteoSense 680®. Note that the fluorescent agent accumulates in the spine and in the kidneys.

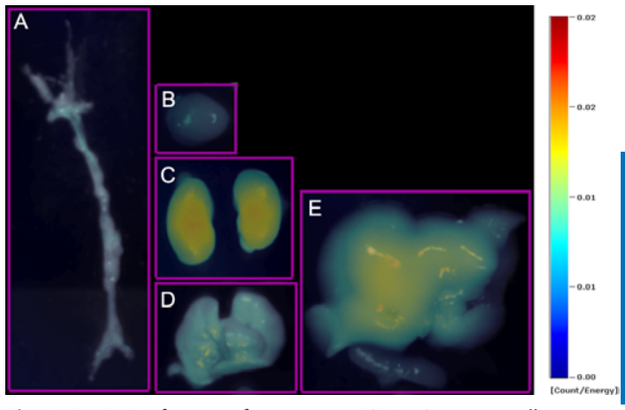

Fig. 9: 2D FMT of organs from an ApoE/FetA-/- mouse. All pictures were taken 24 h after injection of 2 nmol OsteoSense 680®. A) aorta, B) heart, C) kidney, D) lung, E) liver. Note that the strongest fluorescence was detected in the kidneys and in the liver.

Toxicity of Gold Nanoparticles

In collaboration with chemists from RWTH Aachen University and Duisburg-Essen University we continue to study the interaction of live cells and tissues with gold nanoparticles; we determined that gold nanoparticles of diameter 1.4 nm trigger necrosis by oxidative stress and mitochondrial damage [10]. Gold nanoparticles (AuNPs) are generally considered nontoxic, similar to bulk gold, which is inert and biocompatible. AuNPs of

diameter 1.4 nm capped with triphenylphosphine monosulfonate (TPPMS), Au1.4MS, are much more cytotoxic than 15-nm nanoparticles (Au15MS) of similar chemical composition. We studied major cell-death pathways and determined that the cytotoxicity was caused by oxidative stress. Indicators of oxidative stress, reactive oxygen species (ROS), mitochondrial potential and integrity, and mitochondrial substrate reduction were all compromised. Genome-wide expression profiling using DNA gene arrays indicated robust upregulation of stress-related genes after 6 and 12 h of incubation with a twice the IC50 concentration of Au1.4MS, but not with Au15MS nanoparticles. The caspase inhibitor Z-VAD-fmk did not rescue the cells, which suggested that necrosis, not apoptosis, was the predominant death pathway at this concentration. Pretreatment of the nanoparticles with reducing agents/antioxidants N-acetylcysteine, glutathione, and TPPMS reduced the toxicity of Au1.4MS. AuNPs of similar size but capped with glutathione (Au1.1GSH) likewise did not induce oxidative stress. We concluded that besides the size dependency of AuNP toxicity, ligand chemistry is a critical parameter determining the degree of cytotoxicity. AuNP exposure most likely causes oxidative stress that is amplified by mitochondrial damage. Au1.4MS nanoparticle cytotoxicity is associated with oxidative stress, endogenous ROS production, and depletion of the intracellular antioxidant pool.

Selected Publications

[1] C. Lee, E. Bongcam-Rudloff, C. Söllner, W. Jahnen-Dechent, L. Claesson-Welsh (2009) Type 3 cystatins; fetuins, kininogen and histidine-rich glycoprotein. Front Biosci, 14, 2911-2922.
[2] M. Häusler, C. Schäfer, C. Osterwinter, W. Jahnen-Dechent (2009) The physiologic development of fetuin-a serum concentrations in children. Pediatr Res, 66, 660-664.
[3] R. Westenfeld, C. Schäfer, T. Krüger, C. Haarmann, L. J. Schurgers, C. Reutelingsperger, O. Ivanovski, T. Drueke, Z. A. Massy, M. Ketteler, J. Floege, W. Jahnen-Dechent (2009) Fetuin-A protects against atherosclerotic calcification in CKD. J Am Soc Nephrol, 20, 1264-1274.
[4] R. Koos, V. Brandenburg, A. H. Mahnken, G. Mühlenbruch, S. Stanzel, R. W. Günther, J. Floege, W. Jahnen-Dechent, M. Kelm, H. P. Kühl (2009) Association of fetuin-A levels with the progression of aortic valve calcification in non-dialyzed patients. Eur Heart J, 30, 2054-2061.
[5] B. Denecke, S. Gräber, C. Schäfer, A. Heiss, M. Wöltje, W. Jahnen-Dechent (2003) Tissue distribution and activity testing suggest a similar but not identical function of fetuin-B and fetuin-A. Biochem J, 376, 135-145.
[6] N. Tsuchida-Straeten, S. Ensslen, C. Schäfer, M. Wöltje, B. Denecke, M. Moser, S. Gräber, S. Wakabayashi, T. Koide, W. Jahnen-Dechent (2005) Enhanced blood coagulation and fibrinolysis in mice lacking histidine-rich glycoprotein (HRG). J Thromb Haemost, 3, 865-872.
[7] A. Thulin, M. Ringvall, A. Dimberg, K. Kårehed, T. Väisänen, M.-R. Väisänen, O. Hamad, J. Wang, R. Bjerkvig, B. Nilsson, T. Pihlajaniemi, H. Akerud, K. Pietras, W. Jahnen-Dechent, A. Siegbahn, A.-K. Olsson (2009) Activated platelets provide a functional microenvironment for the antiangiogenic fragment of histidine-rich glycoprotein. Mol Cancer Res, 7, 1792-1802.
[8] K. M. Olde Loohuis, W. Jahnen-Dechent, W. van Dorp (2010) The case mid R: milky ascites is not always chylous. Kidney Int, 77, 77-78.
[9] C. N. Rochette, S. Rosenfeldt, A. Heiss, T. Narayanan, M. Ballauff, W. Jahnen-Dechent (2009) A shielding topology stabilizes the early stage protein-mineral complexes of fetuin-A and calcium phosphate: a time-resolved small-angle X-ray study. ChemBioChem, 10, 735-740.
[10] Y. Pan, A. Leifert, D. Ruau, S. Neuss, J. Bornemann, G. Schmid, W. Brandau, U. Simon, W. Jahnen-Dechent (2009) Gold nanoparticles of diameter 1.4 nm trigger necrosis by oxidative stress and mitochondrial damage. Small, 5, 2067-2076.

Marie Curie Practical Training Course organized by HIA - Biointerface
Students and Faculty of the "Marie Curie Cutting Edge Practical Training Course - Tissue engineering, stem cells and biocompatibility testing of biomaterials" held from August 24 – September 3, 2009 at RWTH Aachen. The Marie Curie Program of the European Community fosters early stage training and mobility of researchers. We hosted PhD students and post-Docs from 13 countries. Funding was provided by the European community to the project "InVENTScience" (http://www.inventscience.org).